Supplement of Biogeosciences, 16, 4243–4260, 2019
https://doi.org/10.5194/bg-16-4243-2019-supplement
© Author(s) 2019. This work is distributed under
the Creative Commons Attribution 4.0 License.

Biogeosciences Open Access EGU

Supplement of

Biogeographical distribution of microbial communities along the Rajang River–South China Sea continuum

Edwin Sien Aun Sia et al.

Correspondence to: Moritz Müller (mmueller@swinburne.edu.my)

The copyright of individual parts of the supplement might differ from the CC BY 4.0 License.

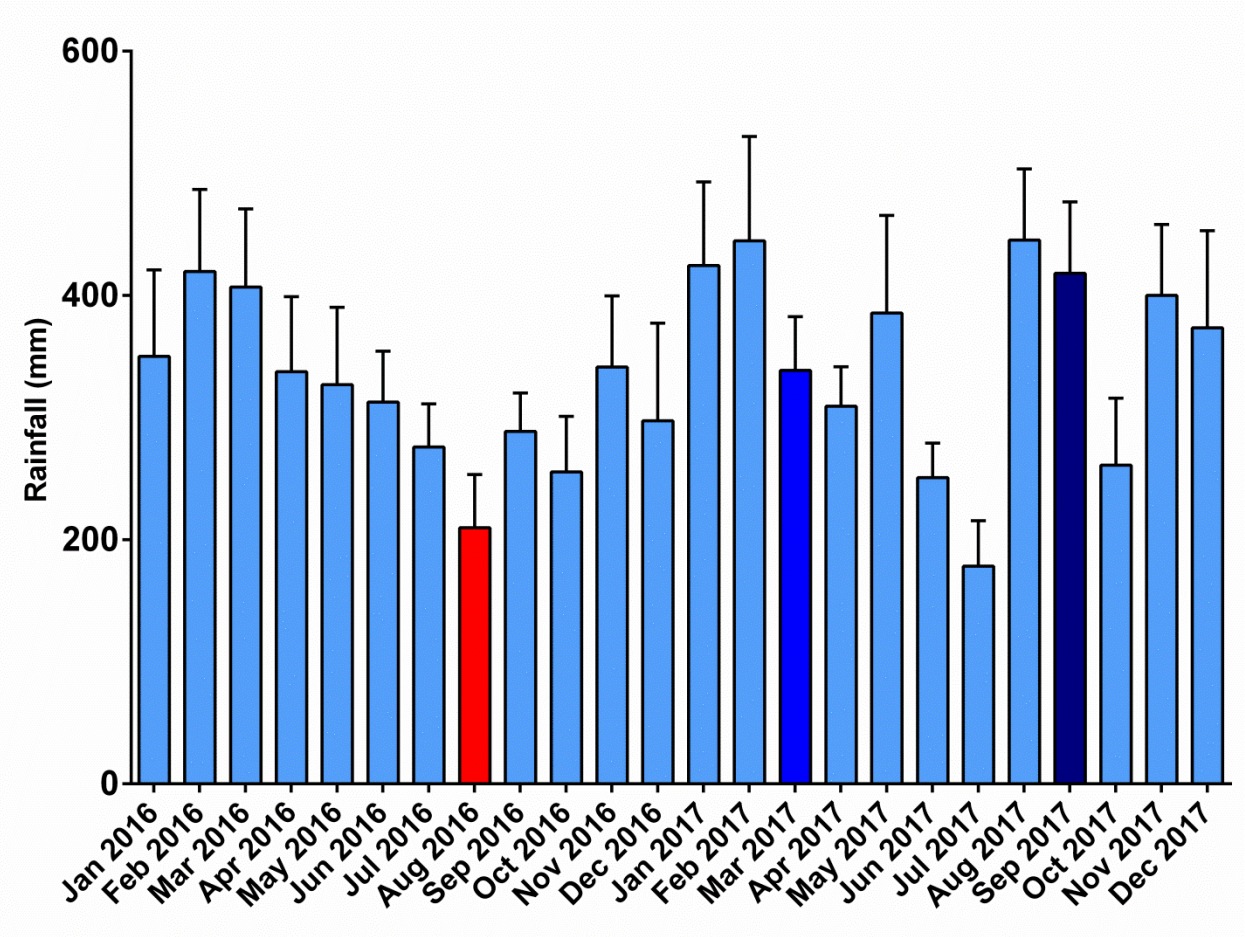

Supp. Fig. S1: Monthly Mean Precipitation (mm) from Jan 2016 to Sep 2017. Relevant months are highlighted red (Aug 2016), blue (Mar 2017) and dark blue (Sep 2017).

Monthly precipitation for the period in between the cruises (August 2016 to September 2017) were obtained from the Tropical Rainfall Measuring Mission website (NASA 2019) in order to gauge the seasonality (wet or dry). As the rainfall data do not correlate with the monsoonal periods, the seasons in which the sampling cruises coincide with were classified based on the mean rainfall that occurred for each month. The August 2016 cruise (colored red) is classified as the dry season based on the lower mean rainfall value as compared to the other two (March 2017 and September 2017), in which the both are classified as the wet season.

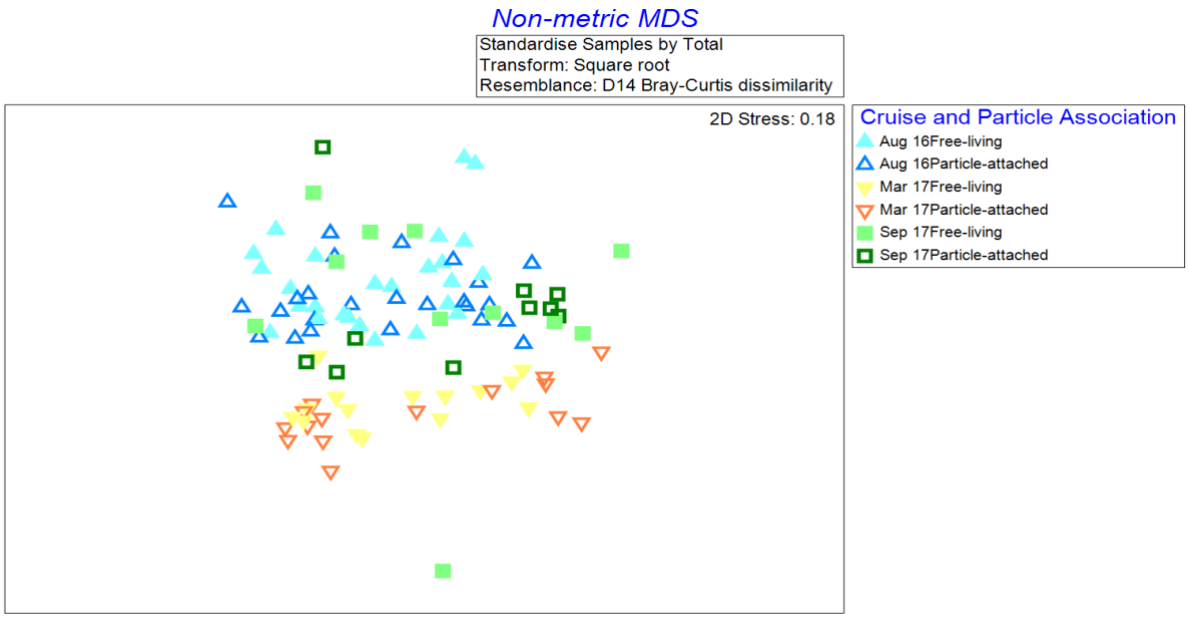

Supp. Fig. S2: Non-metric Multi-dimensional Scaling (NMDS) diagram of seasonal (August 2016, March 2017 and September 2017) and particle association (particle-attached or free-living)

Seasonality was observed within the three cruises irrespective of the particle association (**Supp. Fig. 3**). The August 2016 cruise was found to cluster with the September 2017 whereas the March 2017 cruise clustered separately from the other two cruises. However, it can be seen that there is greater partitioning of free-living and particle-associated samples in the March 2017 samples.

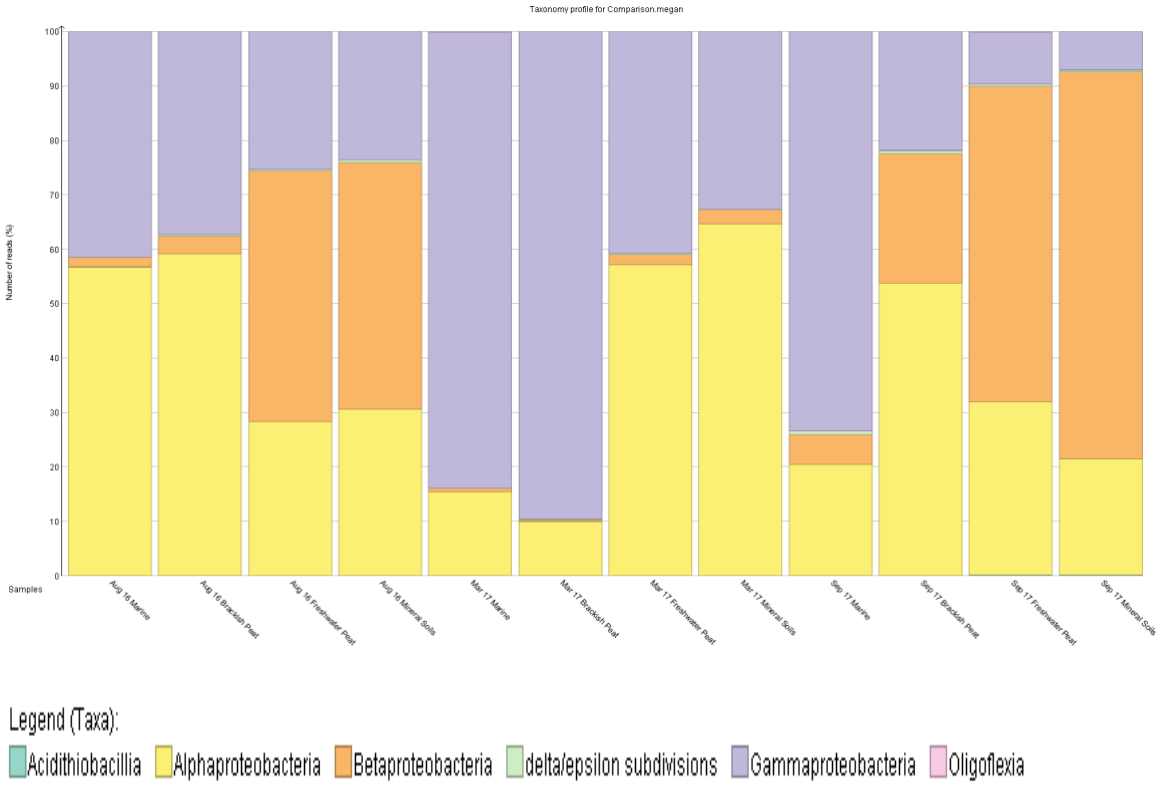

Supp. Fig S3: Relative abundance (%) of dominant classes of *Proteobacteria* along the various source types (Marine, Brackish Peat, Freshwater Peat, Mineral soils) across 3 sampling cruises

The diversity of *Proteobacteria* was examined in more detail as it was the predominant phyla regardless of source type (**Supp. Fig. 4**).In the marine region, the abundance of α-*Proteobacteria* was higher than β-*Proteobacteria*. However, γ-*Proteobacteria* were found to be the predominant class in the marine and brackish peat regions in the March 2017 samples as well as the marine region for the September 2017 samples. It was also shown that the β-*Proteobacteria* was the predominant class of *Proteobacteria* in the August 2016 as well as September 2017 samples. However, in the March 2017 samples the proportion of γ-*Proteobacteria* was greater than that of α-*Proteobacteria* even within the freshwater peat as well as mineral soils region.

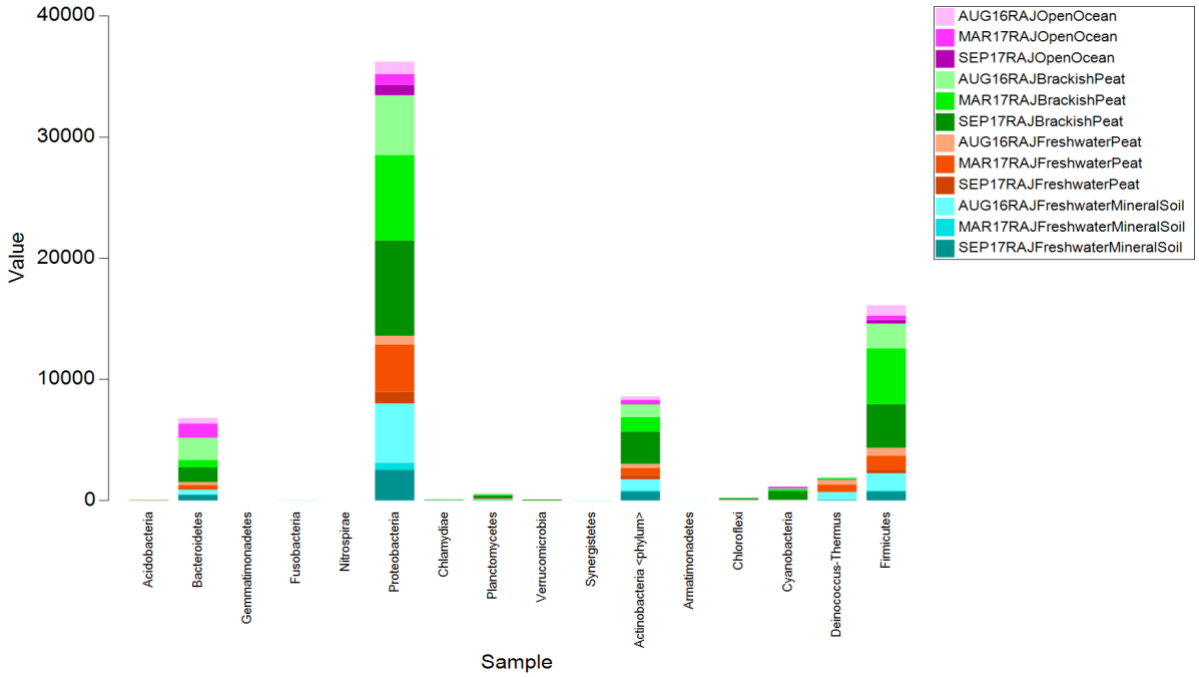

Supp. Fig S4: Absolute values (counts) of the phyla present within all cruises

Based on the information above, the taxonomic data were classified based on the source type (i.e. mineral soil, freshwater peat) in which the stations fall under. According to **Supp. Fig 5**, the bacterial phylum that was the most abundant across all samples was *Proteobacteria* (50.29%), followed by *Firmicutes* (22.35%) and *Actinobacteria* (11.95%). The remaining phyla belonged to *Bacteroidetes* (9.46%), *Deinococcus-Thermus* (2.69%), *Cyanobacteria* (1.61%), *Planctomycetes* (0.84%), *Chloroflexi* (0.34%), *Chlamydiae* (0.14%) and *Verrucomicrobia* (0.11%) respectively. Without taking into consideration the seasonality, spatial variation in the bacterial phyla based on the aforementioned sampling location is evidently apparent which were characteristic for each source types. The combined groups showed that the percentage of the *Proteobacteria* increased from marine (40.78% of total within marine samples), brackish peat (48.96%), freshwater peat (51.86%) to mineral soils (57.59%) while the percentage of *Firmicutes* decreased from marine (24.14%), brackish peat (25.31%), freshwater peat (19.34%), to mineral soils (16.26%). Furthermore, it can be seen that the phylum *Deinococcus-Thermus* generally has a higher relative abundance in freshwater peat (9.28%) as well as mineral soils (5.07%) as compared to marine (0.16%) and brackish peat (0.55%).

The separation of groups was also shown down to the genus level as shown in the heatmap (**Fig 4.6**) whereby the marine and brackish peat groups are distinct from the freshwater peat as well as mineral soil, with the exception of the groups that fall in the marine and brackish peat for September 2017.

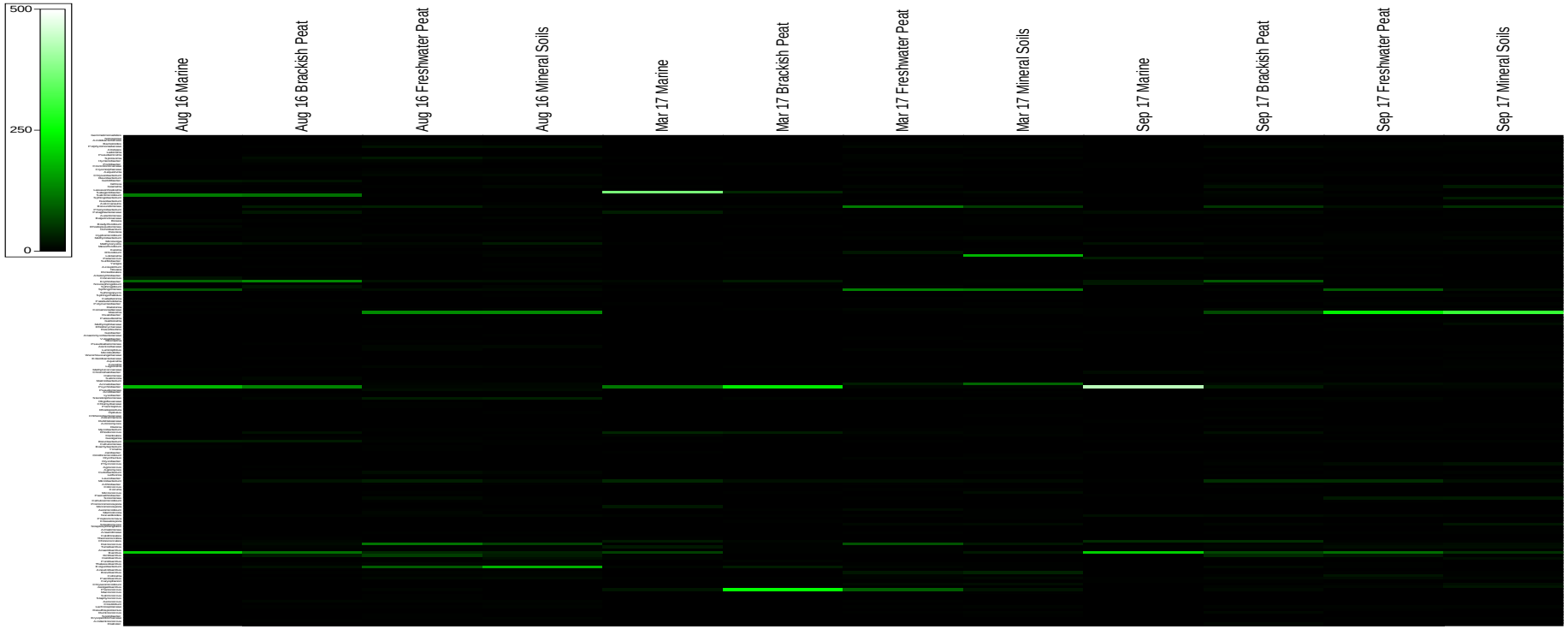

Supp. Fig. S5: Heatmap of the bacterial community composition (OTU reads, genus level). The relative abundance of each taxon is indicated by the intensity of the colour ranging from black (indicative of 0) to white (500) with the green scale as the values in between.

The heatmap also showed different distribution pattern for i) the sampling cruise as well as ii) the different source type. *Salinimicrobium* for example was present in August 2016 in the marine and brackish peat samples but absent from freshwater peat as well as mineral soils. Similar patterns were observed for *Erythrobacter*, *Sphingomonas*, *Psychrobacter*, and *Bacillus*. On the other hand, *Deinococcus*, *Exiguobacterium*, and *Masilia* were the major genera present in freshwater peat and mineral soil.

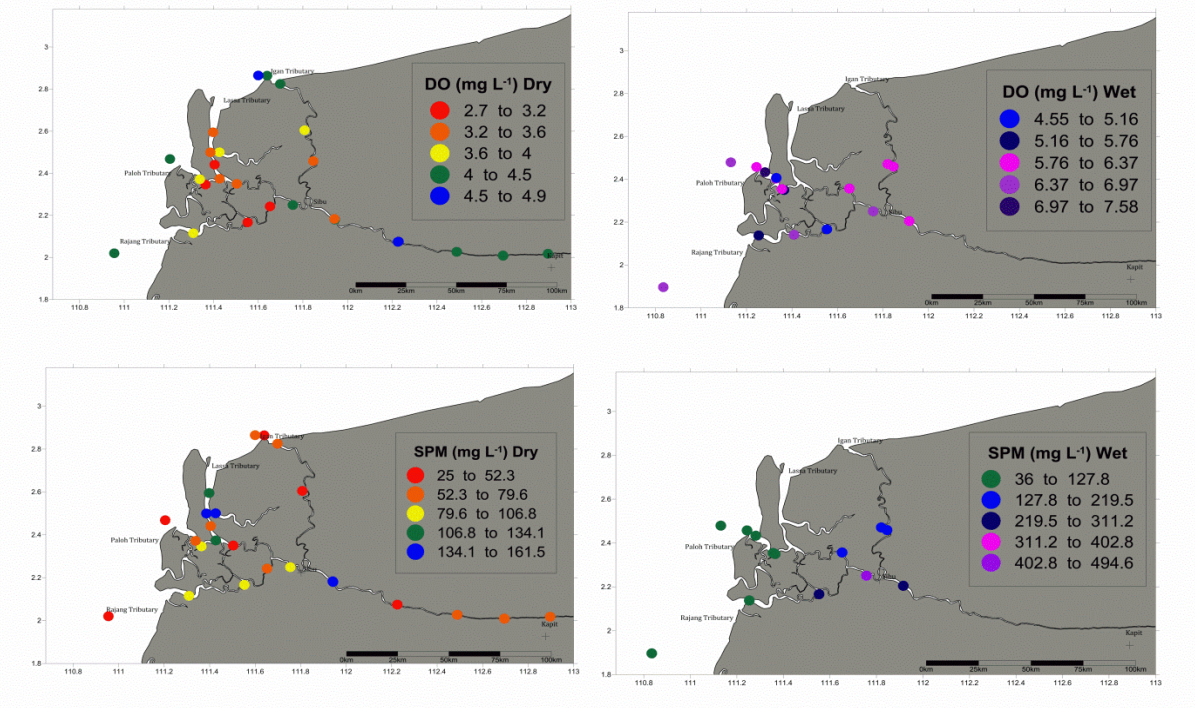

Supp. Fig. S6: Distribution of dissolved oxygen, DO (mg L_1) and suspended particulate matter, SPM (mg L_{-1}) in the dry and wet season along the Rajang River-South China Sea continuum

The picoplankton samples were sent to Institute of Ocean and Earth Sciences, University of Malaya for enumeration. A Flow cytometer (Partec CyFlow Space, Partec, Germany) was used to determine the cell abundance (cells mL^{-1}) of *Prochlorococcus*, *Synechococcus*, and pico-eukaryotes based on their auto-fluorescence of the chlorophyll (FL3 channel), phycoerythrin (FL2 channel) and side scattering characteristics. The average values for each source type was calculated and plotted on a bar graph as shown in **Supp. Fig 8.**

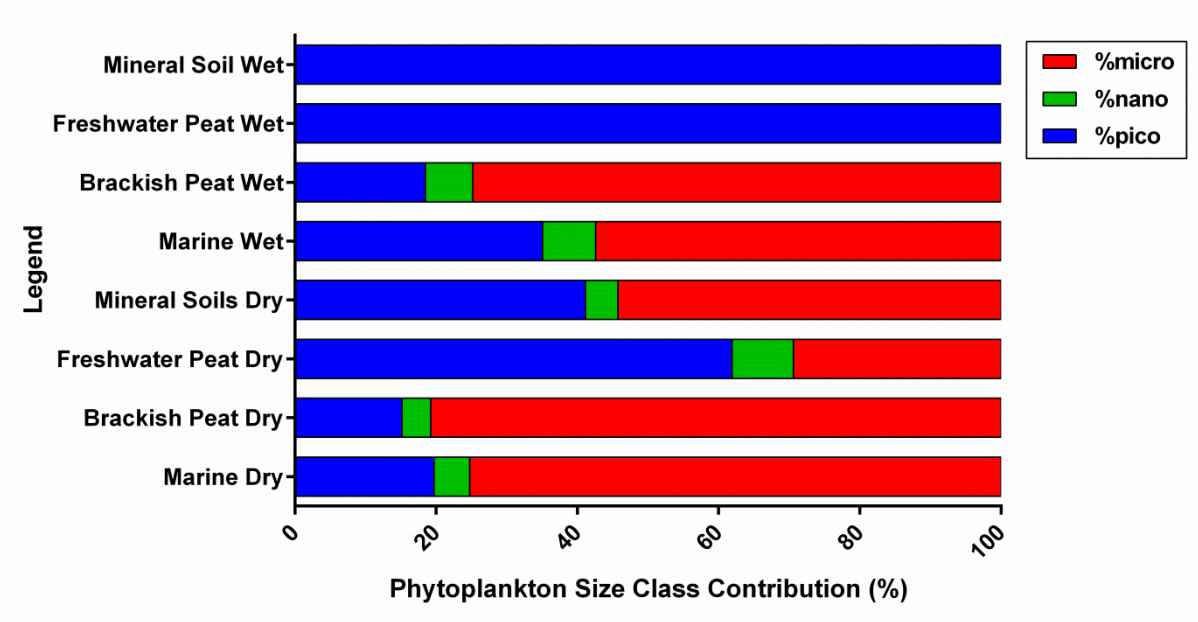

Supp. Fig. S7: Graphical representation of the average relative proportion of phytoplankton size class (%) in both dry and wet seasons according to source type

A venn diagram was plotted based on the MetaCoMET tool (https://probes.pw.usda.gov/MetaCoMET/index.php) to visualize the overlap of particle-association as well as land use as shown in Supp. Fig. 9 and Supp. Fig. 10, respectively.

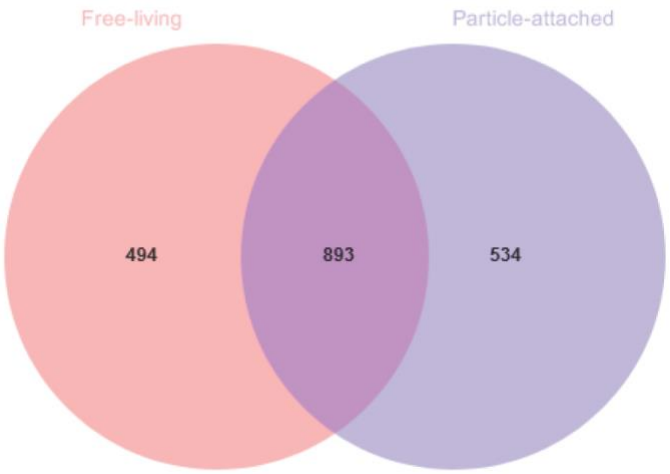

Supp. Fig. S8: Venn diagram of OTU overlapping based on particle association (core microbiome). The red section represents the free-living portion and the purple section represents the particle-attached portion.

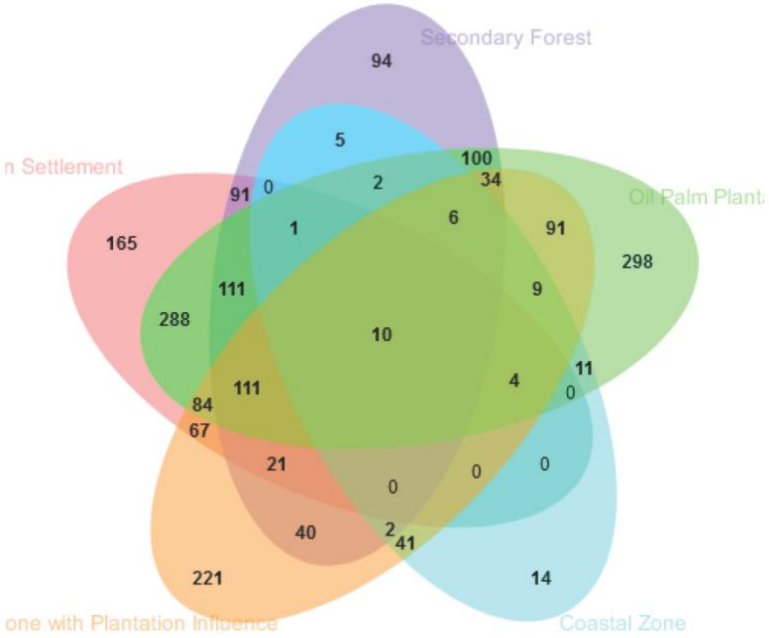

Supp. Fig. S9: Venn diagram of OTU overlapping based on land use classification (core microbiome). The colours representing each land use type are (in anti-clockwise direction): 1)blue: coastal zone; 2) green: oil palm plantation; 3) purple: secondary forest; 4) red: human settlement; 5) orange: coastal zone with plantation influence

Coherence plots (Supp. Fig. 11, Supp. Fig. 12 and Supp. Fig. 13) were plotted based on the Index of Association resemblance with SIMPROF calculations (999 permutations, with significance levels of 5%). Among the the coherence plots generated, several graphs were selected to highlight the taxa that were more apparent in the selected samples that were influenced by anthropogenic activities. The identities of the OTUs were based on the taxonomy table generated from mothur.

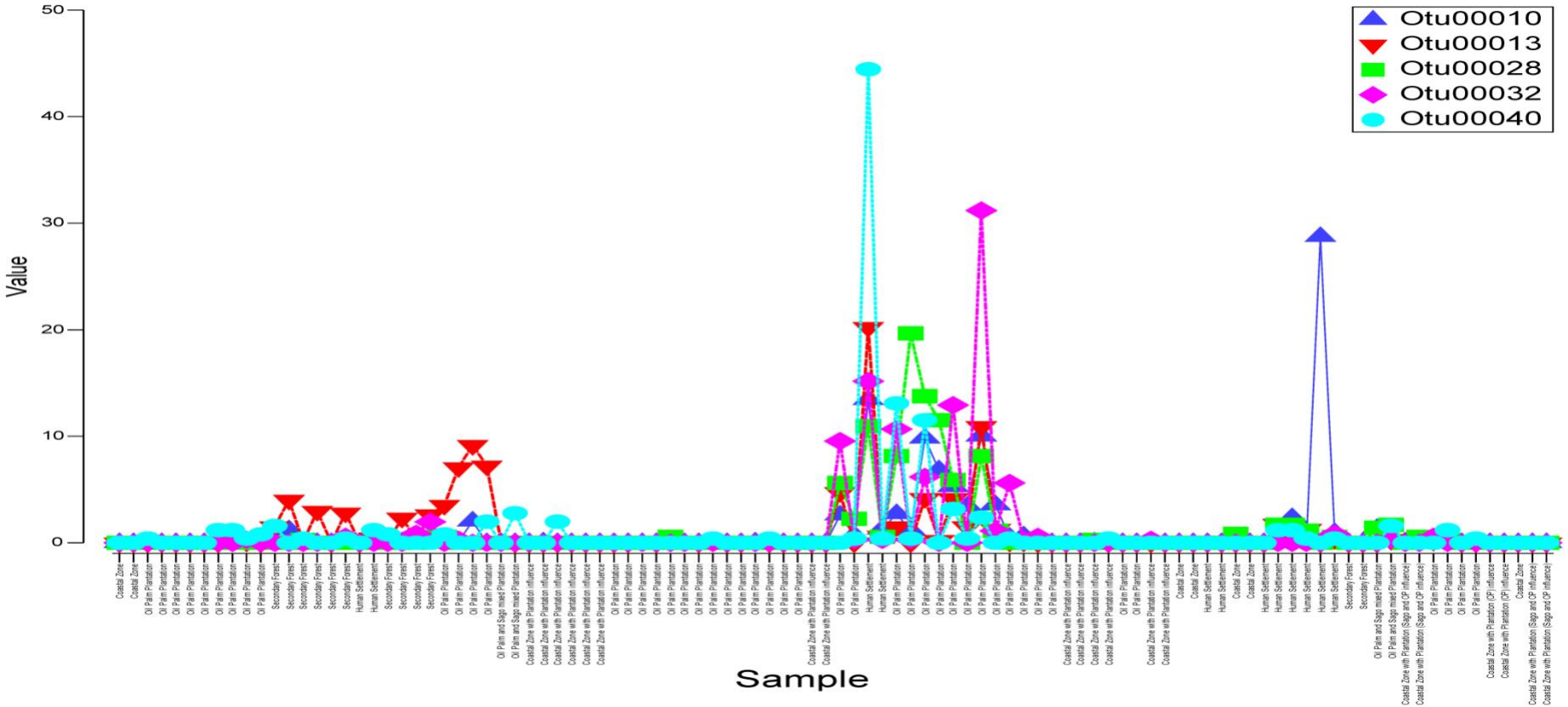

Supp. Fig. S10: Otu00010 (*Proteobacteria; Alphaproteobacteria*), Otu00013 (*Deinococcus-Thermus; Deinococci*), Otu00028 (*Unclassified*), Otu00032 (*Bacteroidetes; Cytophagia*), Otu00040 (*Actinobacteria; unclassified*)

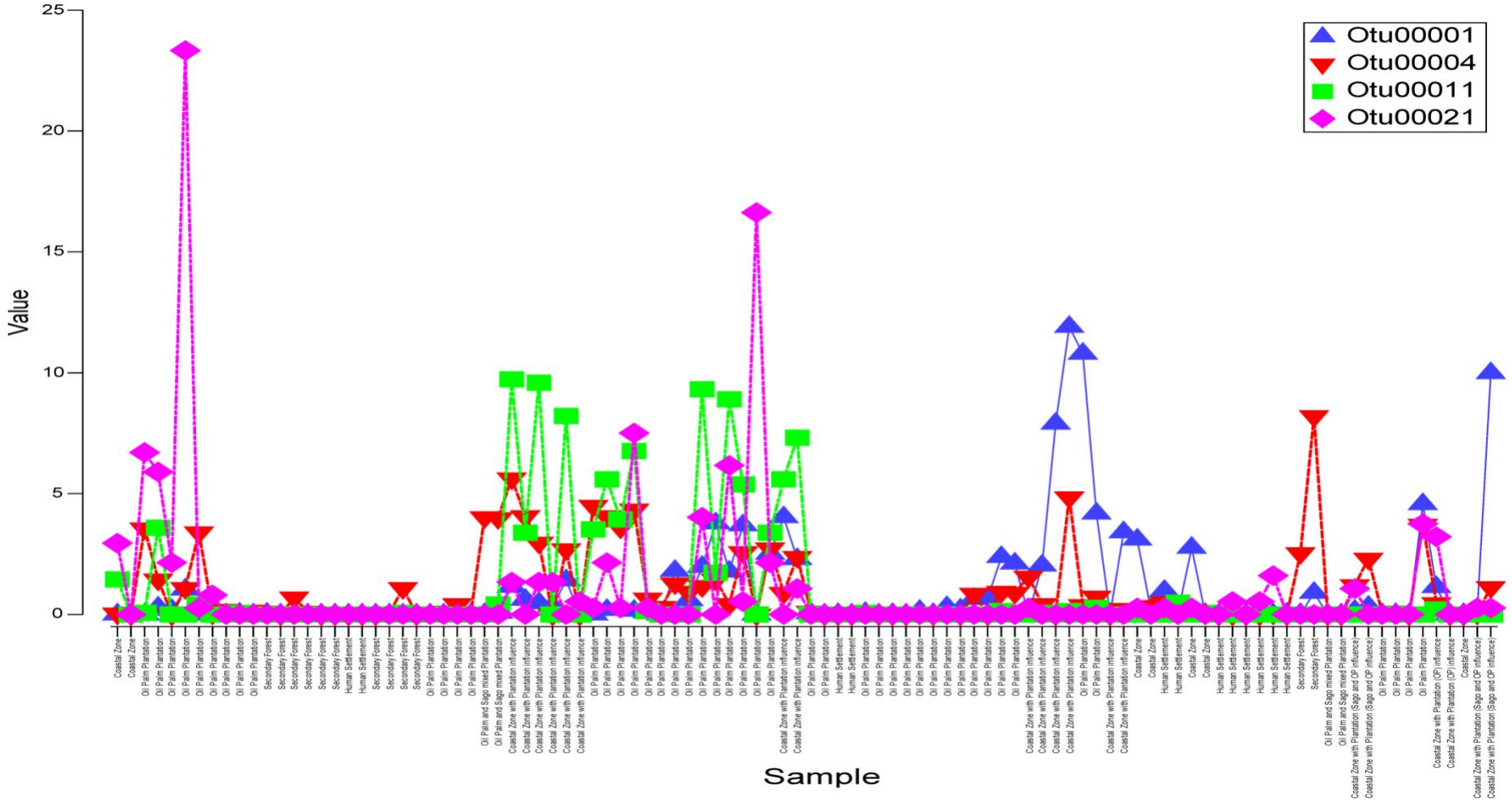

Supp. Fig. S11: Otu00001 (*Proteobacteria; Gammaproteobacteria*), Otu00004 (*Proteobacteria; Alphaproteobacteria*), Otu00011 (*Bacteroidetes; Flavobacteria*), Otu00021 (*Firmicutes; Bacill*

A Euclidean-distance based matrix was constructed based on the physico-chemical parameters of the samples and were plotted against bacterial taxa (Class).

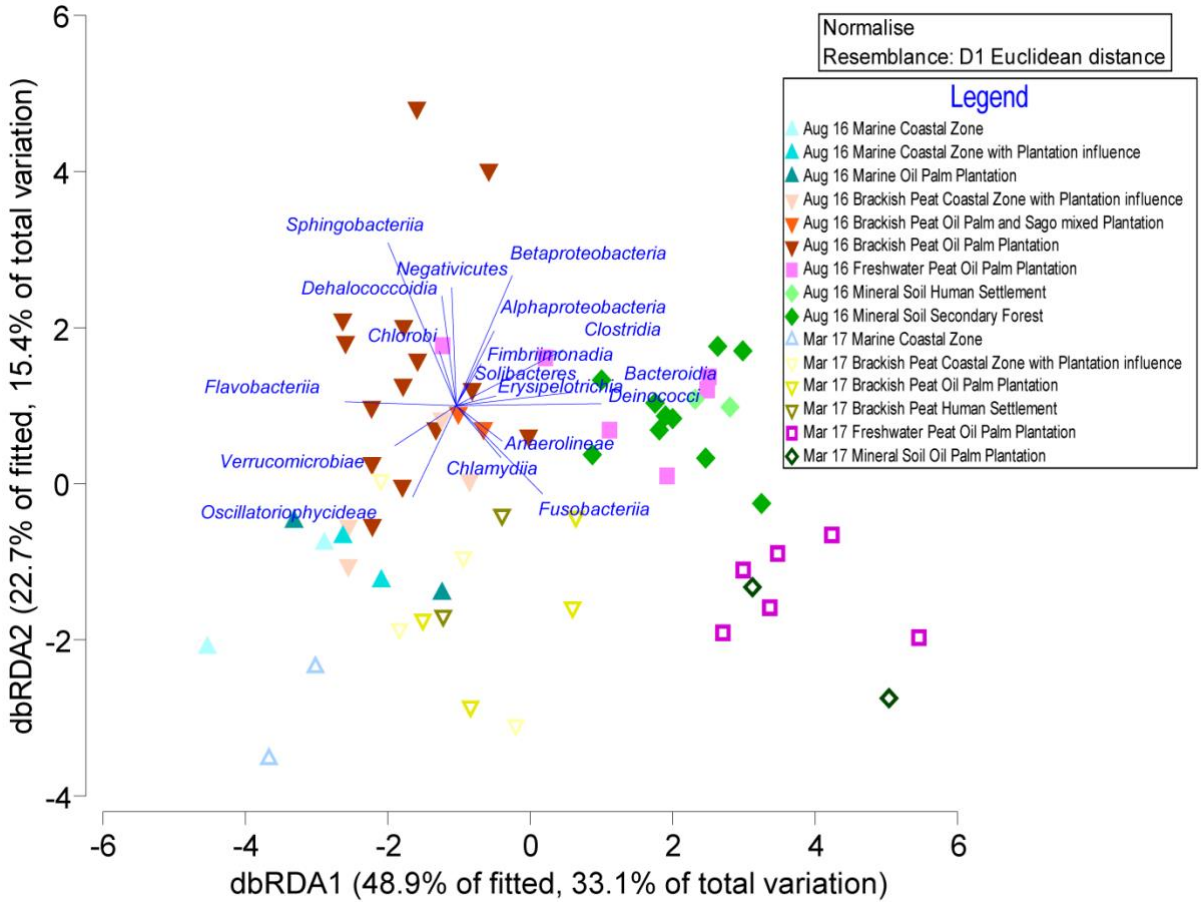

Supp. Fig. S12: Distance-based Redundancy Analysis (dbRDA) plot environmental variables samples based on a linear model (DistLM) of bacterial taxa (Class), shown as vectors. of

Incubation Experiment

Position: Belawai of Rajang River Estuary

Sampling time: 2016-08-28 at 06:00

Original sample was collected from surface with bucket

Water Depth: 6.8 m

Transparency: 60 cm

Samples were passed through a 300 um size mesh and mixed in a tank

Volume of incubation bottle: 1.5 L

Tem (pH)	pH	Tem (DO)	Salinity	DO (mg/l)	DO (%)	DO (mbr)
27.7	7.99	25.8	33.8	4.25	63.2	129.8

Respiration incubation was carried out for 9 hours in both dark and light bottles.

Supp. Table S1: Incubation Experiment

Initial (mg L^{-1})	Bottle	Final Dark (mg L^{-1})	Respiration (g DO L^{-1} D^{-1})	Final Light (mg L^{-1})	Net Primary Productivity (g DO L^{-1} D^{-1})
4.25	**1**	4.18	0.19	4.6	0.51
	2	4.11	0.37	4.41	0.23
	3	3.97	0.75	4.54	0.42
		Average± SE (g DO L^{-1} D^{-1})		**Average± SE (g DO L^{-1} D^{-1})**	
		0.44 ± 016		0.39±0.08	